European Journal of Orthodontics 34 (2012) 655–664
doi:10.1093/ejo/cjr106
Advance Access publication 20 September 2011

The assessment of facial variation in 4747 British school children

Arshed M. Toma*, Alexei I. Zhurov*, Rebecca Playle*, David Marshall**, Paul L. Rosin** and Stephen Richmond*

*Department of Applied Clinical Research & Public Health, Dental School and **School of Computer Science & Informatics, Cardiff University, Wales, UK

Correspondence to: Arshed M. Toma, Department of Applied Clinical Research and Public Health, Cardiff University Dental Hospital—1st Floor, Graduate Room, Heath Park, Cardiff CF14 4XY, Wales, UK. E-mail: TomaA@cardiff.ac.uk

SUMMARY The aim of this study is to identify key components contributing to facial variation in a large population-based sample of 15.5-year-old children (2514 females and 2233 males).

The subjects were recruited from the Avon Longitudinal Study of Parents and Children. Three-dimensional facial images were obtained for each subject using two high-resolution Konica Minolta laser scanners. Twenty-one reproducible facial landmarks were identified and their coordinates were recorded. The facial images were registered using Procrustes analysis. Principal component analysis was then employed to identify independent groups of correlated coordinates.

For the total data set, 14 principal components (PCs) were identified which explained 82 per cent of the total variance, with the first three components accounting for 46 per cent of the variance. Similar results were obtained for males and females separately with only subtle gender differences in some PCs.

Facial features may be treated as a multidimensional statistical continuum with respect to the PCs. The first three PCs characterize the face in terms of height, width, and prominence of the nose. The derived PCs may be useful to identify and classify faces according to a scale of normality.

Introduction

Facial morphology attracts interest from a wide variety of research disciplines (e.g. anthropology, developmental anatomy, genetics, maxillofacial surgery, cosmetic surgery, orthodontics, and psychology). The three-dimensional (3D) analysis of facial soft tissues has potential for the identification of morphological features and changes in these features as a result of growth and clinical interventions (McCance *et al.*, 1992; Ferrario *et al.*, 1998a,b, 1999; Nute and Moss, 2000; Hennessy and Moss, 2001; Moss *et al.*, 2003; Kau and Richmond, 2008).

Recent research has focused on facial landmark variation particularly in genetic and medical disorders (Hennessy *et al.*, 2002, 2004, 2007, 2010; Hammond *et al.*, 2004, 2005). There are many theories of facial growth and irrespective of the theory, development of the face can be influenced by advantageous or adverse events particularly during the gestation period extending into early childhood. The genetic and environmental interactions may result in minor physical anomalies affecting the relative position of facial landmarks.

However, the differences in the anatomical position of facial landmarks are usually very subtle and difficult to recognize by subjective examination alone. There are a number of algorithms available that evaluate 3D facial landmarks, which are commonly affected in craniofacial syndromes (Shaner *et al.*, 2000; Bugaighis *et al.*, 2010). The relative position of facial landmarks has been effectively used to identify some genetic disorders including Williams, Smith-Magenis, 22q11 deletion, and Noonan syndromes (Hammond *et al.*, 2004, 2005).

Although there has been significant attention to 3D assessment of discrete craniofacial anomalies, less attention has been paid to assess normal variation in a population.

The aim of the study is to identify key components contributing to facial variation in a large population-based sample of 15.5-year-old children (2514 females and 2233 males).

Subjects and methods

The children involved in this study were recruited from the Avon Longitudinal Study of Parents and Children (ALSPAC), which was designed to explore how the individual's genotype interacts with different environmental factors to influence health, behaviour, and development of children (Golding *et al.*, 2001). The initial ALSPAC sample consisted of 14 541 pregnancies. This was the number of pregnant women enrolled in the ALSPAC study with an estimated date of delivery between April 1991 and December 1992. Out of the initial 14 541 pregnancies, all but 69 had known birth outcome. Of these 14 472 pregnancies, 195 were twins, 3 were triplets, and 1 was a quadruplet pregnancy; meaning that there were 14 676 fetuses in the initial ALSPAC sample. Of these 14 676

fetuses, 14 062 were live births and 13 988 were alive at 1 year.

The cohort was recalled when the children aged 15.5 years. Invitations were sent to 9985 participants who reported that they were interested to take part in the clinics.

Ethical approval for this study was obtained from the ALSPAC Law and Ethics Committee and the Local Research Ethics Committees.

3D facial scans of the children were taken using two high-resolution Konica Minolta VI-900 laser scanners, 'Konica Minolta Sensing Europe, Milton Keynes, UK'. The cameras were fitted with lenses of focal length 14.5 mm and were connected in serial via a Small Computer System Interface cable to a desktop computer workstation. The scanning of each participant took approximately 8 seconds. The set of left and right facial scans of each individual were processed, registered, and merged using a locally developed algorithm implemented as a macro in 'Rapidform® software; INUS Technology Inc., Seoul, South Korea' (Kau *et al.*, 2004; Zhurov *et al.*, 2005; Toma *et al.*, 2008; Kau and Richmond, 2010).

Twenty-one soft tissue landmarks as defined by Farkas (1994) were manually identified on each facial shell using Rapidform® software (Figure 1). The *x*, *y*, and *z* coordinates of each landmark were recorded (63 coordinates in total). The reproducibility of these landmarks in the *x*, *y*, and *z* dimensions has been previously investigated and the majority showed an error of less than 1 mm for both intra- and inter-examiner assessments (Toma *et al.*, 2009).

Statistical analysis

All facial shells were initially normalized to natural head posture with the origin set at mid-endocanthion point (Figure 2), the *x*-axis pointing left, from right to left eye; *y*-axis pointing vertically upwards, from chin to forehead; *z*-axis pointing outwards, in the nose direction; and the coronal, sagittal, and transverse planes were taken as the xy, yz, and xz planes, respectively (Toma *et al.*, 2009; Zhurov *et al.*, 2010).

Generalized Procrustes analysis was performed to register (align) the sets of 21 facial landmarks by removing translation and rotation (Bookstein, 1991). Scaling was not performed to preserve face size. A centroid representing the mean position for each of the 21 clusters of landmarks was derived. In total, there were 21 centroids. The standard deviations around each centroid were calculated for all individuals and plotted as ellipsoids (Figure 3). Each ellipsoid covers 2 SDs from the mean in *x*, *y*, and *z*, i.e. representing 95 per cent of the variability.

Principal component analysis (PCA) was then employed to identify relatively important correlated variables (Pearson, 1901; Hammond *et al.*, 2004, 2005). The 'Kaiser–Guttman criterion' (Guttman, 1954; Cliff, 1988; Jackson, 1993) was used as the stopping rule to identify critical principal components (PCs). According to this rule, the PCs with eigenvalues greater than the average eigenvalue should only be retained. The rotation method used for PCA was varimax with Kaiser normalization (Kaiser, 1958).

Visualizing facial variation

Average faces were constructed using a locally developed algorithm (Zhurov *et al.*, 2010) implemented as a Rapidform® macro. Parameters characterizing the first PCs, which describe the majority of facial variation, were derived (see the end of the Results) and all faces were split into seven groups in each of the parameters, corresponding to −3 through +3 SDs from the mean value. All facial shells were

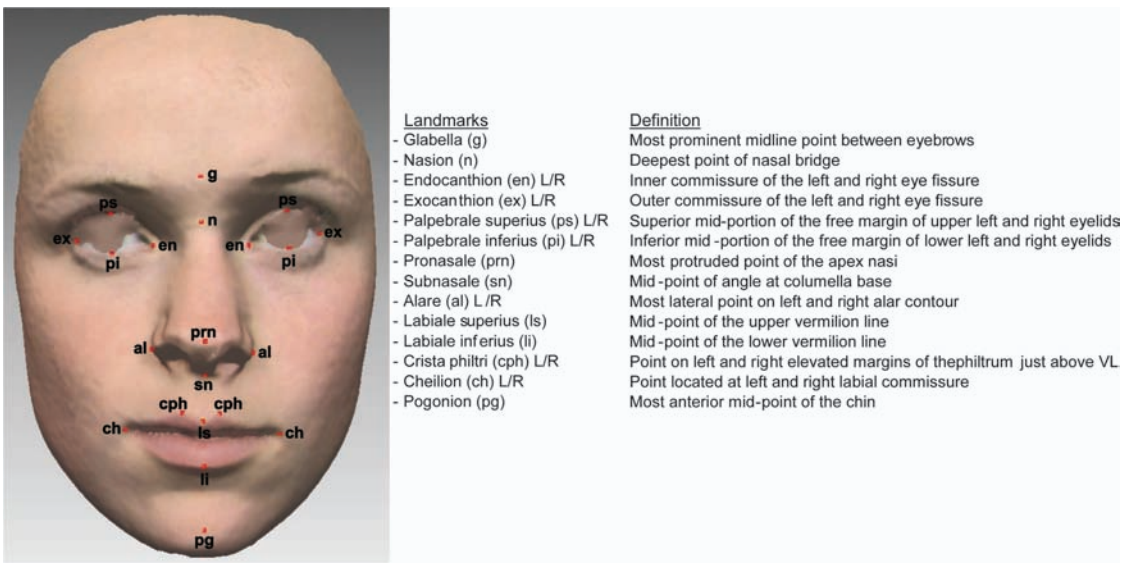

Figure 1 Facial soft tissue landmarks.

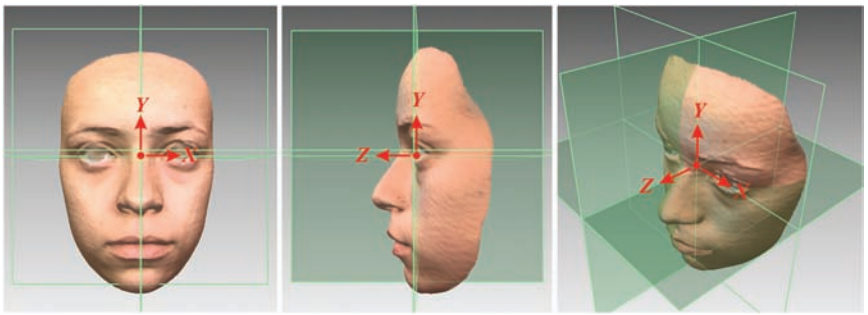

Figure 2 Normalization of facial shells to natural head posture; the *x*-axis (horizontal); *y*-axis (vertical); *z*-axis (depth of field); the coronal, sagittal, and transverse planes were taken as the xy, yz, and xz planes, respectively.

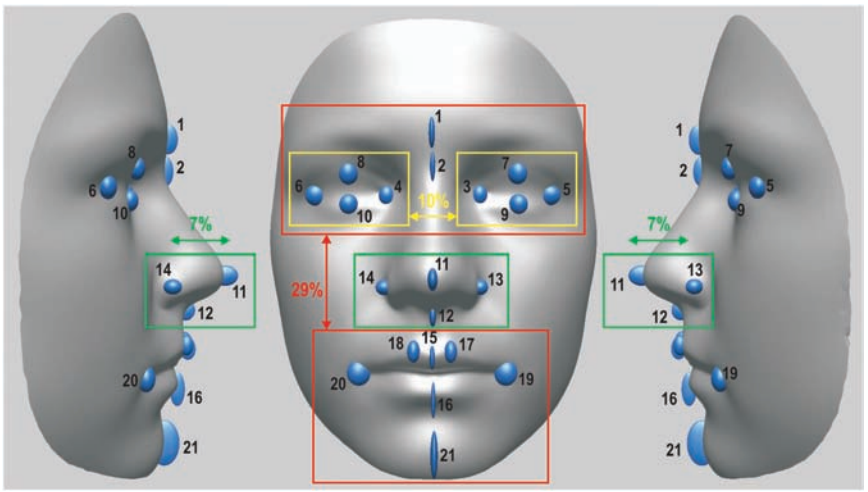

Figure 3 Standard deviation envelopes for 21 facial landmarks, highlighting facial morphology variation revealed by the first three principal components (PCs): PC1 (red, explains 29% of total variance), PC2 (yellow, 10%), and PC3 (green, 7%). 'Facial landmarks': 1, glabella; 2, nasion; 3 and 4, endocanthion (left and right); 5 and 6, exocanthion (left and right); 7 and 8, palpebrale superius (left and right); 9 and 10, palpebrale inferius (left and right); 11, pronasale; 12, subnasale; 13 and 14, alare (left and right); 15, labiale superius; 16, labiale inferius; 17 and 18, crista philtri (left and right); 19 and 20, cheilion (left and right); 21, pogonion.

aligned so that their mid-endocanthion points coincide as well as the sagittal, coronal, and transverse planes.

Results

A total of 5253 children attended the recall clinic. There were 506 individuals out of this sample, which were excluded due to not having their facial images recorded at the time of attending the clinic, poor quality facial scans, obvious ethnicity, and obvious facial dysmorphology. The sample represented normal variation in 4747 Caucasian children (2514 females and 2233 males). The ellipsoid envelopes of variation for the 21 facial landmarks are displayed in Figure 3. The pogonion showed the largest variation in the *y* and *z* axes, whereas the inner canthi and the left and right alari exhibited the least variation.

For the total sample, 14 PCs were identified by PCA (Table 1). This table lists the factor loadings (coefficients) for each coordinate in all extracted PCs. These coefficients indicate the relative importance of different landmark coordinates to the variation identified by each component. Each component includes a group of landmark coordinates (highlighted cells) that have high loadings (coefficients >0.5 in magnitude) in the rotated component matrix. These landmark coordinates contribute greatly to the variation identified by each component. The non-highlighted cells within each component (coefficients < 0.5 in magnitude) indicate landmark coordinates that have less effect on facial variation (coefficients in the range 0.1–0.49 in magnitude are presented and coefficients < 0.1 in magnitude are not shown).

The 14 PCs explain 82.1 per cent of the total variance in facial form (Table 2), with the first three components

Table 1 Principal component analysis of landmark data—4747 individuals. PC, principal component

PC	*X–Y–Z*	PCs													
		1	2	3	4	5	6	7	8	9	10	11	12	13	14
PC1	lsY	**−0.851**		0.260							0.186				
	cphRY	**−0.843**		0.243			0.102				0.126				
	cphLY	**−0.841**		0.240			0.107				0.137				
	enLY	**0.834**	0.138	−0.112	0.165	−0.200	−0.155								−0.105
	enRY	**0.829**	0.160	−0.108	0.153	−0.176	−0.180						0.106		0.116
	pgY	**−0.822**	−0.155				−0.187								
	chRY	**−0.816**	−0.190		−0.214										
	chLY	**−0.814**	−0.180		−0.221			−0.100						−0.121	
	piRY	**0.810**			0.154	−0.151	−0.256						0.125	−0.100	0.168
	piLY	**0.808**			0.165	−0.170	−0.254						−0.137	−0.104	−0.162
	psLY	**0.792**					−0.278						−0.123	0.332	−0.126
	psRY	**0.783**					−0.276						0.112	0.335	0.181
	liY	**−0.769**	−0.124		−0.386										
	exRY	**0.759**			0.189	−0.210	−0.309						0.145		0.197
	exLY	**0.748**			0.194	−0.173	−0.313						−0.184		−0.220
	gY	**0.644**	0.223			0.308	−0.130					−0.192			
	nY	**0.620**	0.132	−0.468		0.123						−0.145			
PC2	psLX	0.143	**0.939**						−0.125						
	psRX	−0.139	**−0.939**						−0.116						
	piLX	0.144	**0.933**						−0.135						
	piRX	−0.150	**−0.932**						−0.127				−0.126		
	enRX		**−0.837**			0.129			−0.168					0.219	
	enLX	0.102	**0.830**			−0.108			−0.126					−0.225	
	exRX	−0.192	**−0.810**					0.123				−0.116		−0.391	
	exLX	0.184	**0.768**					−0.123	−0.148			0.140		0.432	
PC3	alLZ	0.209		**−0.798**		−0.101	−0.171	−0.130				−0.136			
	alRZ	0.220		**−0.786**			−0.152	−0.144				−0.132			
	snZ	0.347		**−0.706**	0.260	−0.144		−0.150				−0.113			
	prnZ	0.404		**−0.690**		−0.253	−0.138	−0.204				−0.185			
	liZ	0.295		**0.562**				−0.239							
PC4	lsZ	0.368			**0.863**			−0.102			−0.163				
	cphRZ	0.391			**0.861**	−0.112		−0.110							
	cphLZ	0.388			**0.861**	−0.117							−0.109		
	pgZ	−0.151		0.271	**−0.788**		−0.195	−0.321							
PC5	gZ	−0.103	0.198	0.176		**−0.858**						−0.148		0.158	
	nZ		0.157	−0.163		**−0.822**	0.103					−0.299		0.167	
	piRZ	−0.374		0.352	−0.245	**0.673**					0.114	−0.120			
	piLZ	−0.376		0.349	−0.242	**0.659**			0.117		0.105	−0.111	0.119		
	enLZ	−0.469		0.244	−0.191	**0.521**	0.154		0.111			−0.139		0.274	
	enRZ	−0.458		0.250	−0.185	**0.485**	0.167			−0.105		−0.140		0.321	
PC6	prnY					0.120	**0.821**					0.106			
	alLY	−0.284					**0.791**		−0.108						
	alRY	−0.299					**0.768**								
	snY	−0.226		0.184			**0.722**					0.162			
PC7	chRX	−0.123	−0.128					**0.835**			0.196				
	chLX	0.139	0.145					**−0.821**			−0.205				
	chLZ	0.203		0.230				**0.814**					−0.124		
	chRZ	0.195		0.225				**0.806**					0.145		
PC8	snX								**0.940**						
	prnX								**0.906**	0.167					−0.139
PC9	gX									**0.974**					
	nX									**0.967**					
PC10	cphRX	−0.164						0.183			**0.809**		0.312		
	cphLX	0.147						−0.199			**−0.768**		0.422		
	alLX	0.266	0.321		0.158	−0.163		−0.219	0.266		**−0.488**	0.188			
	alRX	−0.275	−0.332		−0.162	0.158		0.219	0.265		**0.481**	−0.189			
PC11	psLZ	−0.275		0.207		0.101	0.219		0.109			**0.805**	0.109		
	psRZ	−0.288		0.237			0.209		−0.116			**0.784**	−0.125		
PC12	lsX												**0.942**		
PC13	exLZ	−0.307	−0.252	0.278	−0.172	0.369			0.166	0.105			0.161	**−0.618**	
	exRZ	−0.320	−0.290	0.287	−0.186	0.368	0.109		−0.129	−0.118			−0.146	**−0.598**	
PC14	pgX								−0.180				−0.153		**0.926**
	liX								−0.104				0.486		**0.775**

The highlighted cells (coefficients >0.5 in magnitude) indicate landmark coordinates that contribute greatly to the facial variation; non-highlighted cells (coefficients <0.5 in magnitude) indicate landmark coordinates that have less effect on facial variation (coefficients in the range 0.1–0.49 in magnitude are presented and coefficients <0.1 in magnitude are not shown).

Table 2 Brief description of the principal components (PCs) extracted for the total sample and their corresponding positions in male and female samples

Total sample (N = 4747)		Males (N = 2233)		Females (N = 2514)	
Brief description of PCs	Percentage of variance	PC	Percentage of variance	PC	Percentage of variance
PC1, face height	28.8	PC1	24.2	PC1	21.9
PC2, inter-eye distance (face width)	10.4	PC2	11.0	PC2	11.1
PC3, prominence of the nose	6.7	PC3	7.4	PC3	7.6
PC4, protrusion of the upper lip relative to the chin	5.3	PC4	5.4	PC4	5.7
PC5, eye depth relative to the nasal bridge	4.8	PC6	4.5	PCs 7 and 9	4.4 + 3.3
PC6, vertical height of the nose	4.4	PC5	5.1	PC6	4.4
PC7, ratio of the mouth width to mouth depth	4.0	PC7	4.4	PC5	5.0
PC8, deviation of the nasal tip and columella base	3.6	PC8	3.8	PC8	3.9
PC9, horizontal asymmetry of the nasal bridge	3.2	PC10	2.7	PC10	2.9
PC10, philtrum-to-nose width ratio	2.7	PCs 14 and 15	1.8 + 1.7	PCs 15 and 16	1.7 + 1.6
PC11, Upper eyelid depth	2.4	PC12	2.3	PC13	2.0
PC12, horizontal asymmetry of the upper lip (philtrum)	2.3	PC11	2.5	PC11	2.7
PC13, Facial flatness (outer canthi depth)	1.9	PC9	3.4	PC14	1.8
PC14, horizontal asymmetry of the chin and lower lip	1.7	PC13	2.0	PC12	2.4

The order of PCs (1–14) for the total sample is based on their percentage of variance (descending order), PC1 has the highest percentage of variance and PC14 has the least percentage of variance. PCs 14 and 15 (males) describe variation in philtrum and nose width, respectively; PCs 7 and 9 (females) describe variation in depth of the lower eyelids (relative to the nasal bridge) and inner canthi, respectively; PCs 15 and 16 (females) describe variation in nose and philtrum width, respectively. Examples: PC6 (total sample) explains variation of the vertical height of the nose is positioned as PC5 (males) and PC6 (females); PC7 (total sample) explains variation of the mouth width to mouth depth ratio is positioned as PC7 (males) and PC5 (females).

accounting for 45.9 per cent of the total variance (PC1 28.8 per cent, PC2 10.4 per cent, and PC3 6.7 per cent). The other PCs account for considerably smaller portions of the total variance (PC4 5.3 per cent, PC5 4.8 per cent, PC6 4.4 per cent, etc.).

The first PC includes two subsets of landmarks grouped around the eyes and mouth (highlighted by red rectangles in Figure 3). The first subset represents the y coordinates of 10 upper face landmarks including eight landmarks around the eyes (3–10) as well as glabella and nasion. The second subset includes the y coordinates of seven lower face landmarks (15–21). The loadings of the two subsets have opposite signs; this indicates statistical variation in opposite (upward–downward) directions. Therefore, PC1 essentially describes variation in face height.

The second PC (enclosed in yellow rectangles) consists of the x coordinates of eight landmarks around the eyes (3–10). Loadings with opposite signs correspond to variation in opposite (outward–inward) directions. Therefore, this component essentially describes variation in inter-eye width.

The third PC (indicated by green rectangle) represents a single group of the z coordinates of four landmarks associated with the nose (11–14); consequently, this component characterizes the prominence of the nose.

PCA was also applied when the data set was separated out into males and females. Fifteen PCs were identified for males and 16 for females. Brief component definitions and variances explained are listed in Table 2. The first eight PCs for males and the first four components for females were roughly the same as those of the total sample. Subtle gender differences were noticed in the sequence of some PCs as compared with the total sample; for example, PC14 (related to asymmetry of the chin in the total sample) was positioned as PC13 and PC12 in males and females, respectively.

Visualizing facial variation

A total of 21 average faces were constructed to visualize facial morphology variation identified by the first three PCs (Figure 4). Three parameters (P1, P2, and P3) characterizing the first three PCs were defined as follows:

- P1: vertical distance between the centroids of the upper and lower sets of landmarks (1–10 and 15–21);
- P2: horizontal distance between the centroids of the left and right sets of landmarks associated with the eyes;
- P3: z coordinate of the centroid of the landmarks associated with the nose (11–14).

The facial variation identified by the first three PCs is presented visually in this section as these components explained the majority of the variation and it is shown as an example that the principle can be applied to all 14 components.

Discussion

Fifty-three per cent of the invited children attended the recall, and 90 per cent of these had suitable facial scans. The present study assessed normal variation of facial morphology in a large population-based cohort of Caucasian adolescents 15.5 years of age. The results can be considered specific to

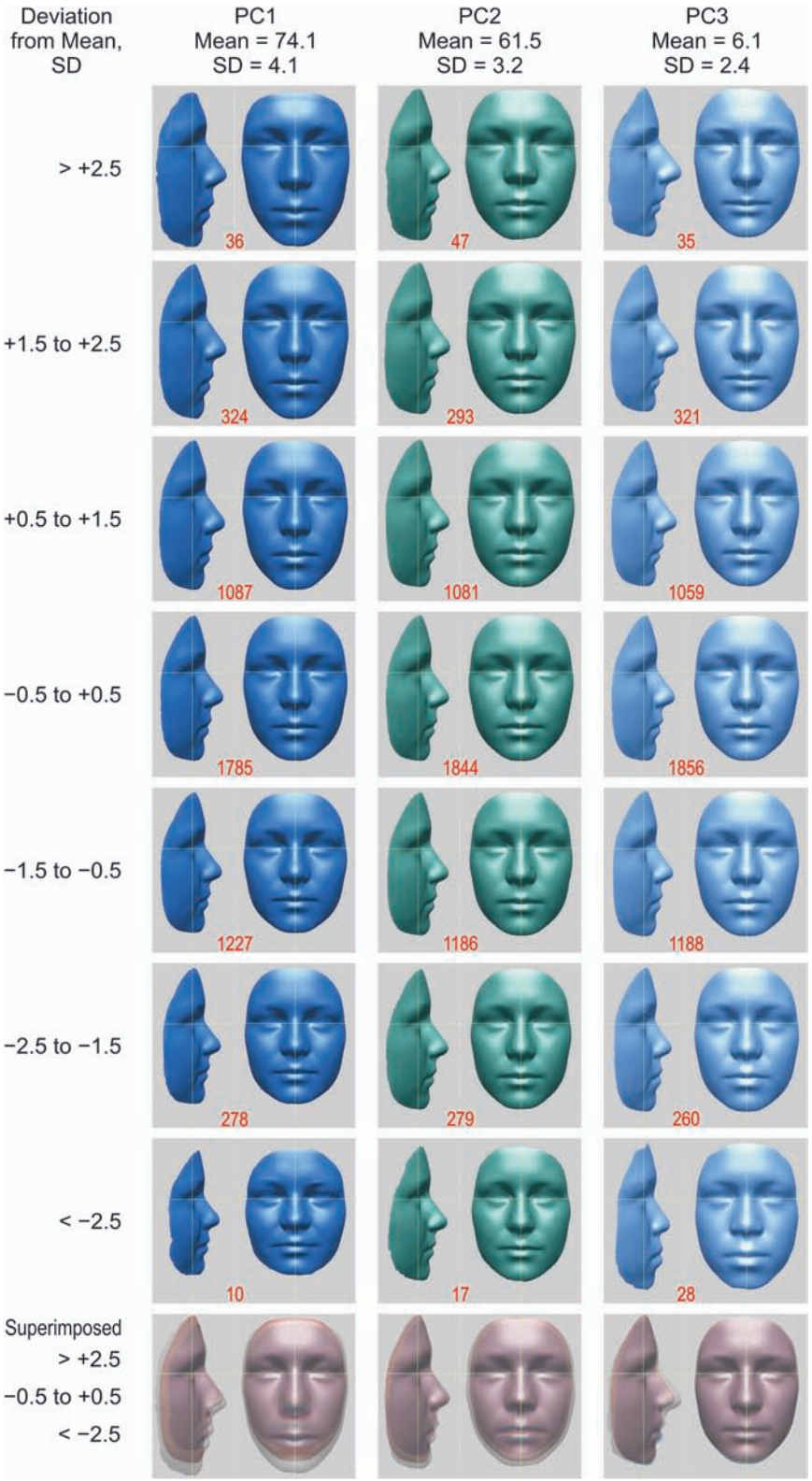

Figure 4 Average faces constructed to illustrate variation in face height (left column, PC1), inter-eye distance (middle column, PC2), and prominence of the nose (right column, PC3). The numbers shown in red colour represent the number of individuals contributed to each average face.

this particular population, and the methodology used in this study can form the basis to analyse and compare facial morphology of other population groups.

The 3D acquisition technique used in this study is laser scanning; the accuracy of surface scanning with Konica Minolta 900/910 laser scanners is in the range of 0.3–0.5 mm, whereas the images obtained with a photogrammetry approach such as 3dMD (Atlanta, GA) cameras have been reported as 0.8–1.0 mm (Kau *et al.*, 2005). The laser scanner has sufficient surface resolution to detect the detailed morphology, particularly the fine lines that form the inner and outer canthi. However, the capture time of the 3dMD system is 1.5 milliseconds at the highest resolution compared to approximately 8 seconds scanning time using laser scanners. Therefore, the laser scanning requires a protocol to instruct the patient to remain still, presenting with no facial expressions.

Although the acquisition time for the laser cameras is relatively long, the reliability of this technique is remarkably good over a 3 day period (Kau *et al.*, 2005). Both Konica/Minolta 900/910 and the photogrammetry techniques use colour texture overlays, and the resolution of the colour texture is superior using photogrammetry compared with the laser technique. However, achieving consistent colour balance is difficult and often the colour tones can mask facial contours and in this study the colour texture was not applied.

Fourteen PCs were identified describing the majority of facial soft tissue variation (82 per cent), with the first three components accounting for 46 per cent of the total variance. The sample was registered using Procrustes analysis; with this technique, the landmark 3D coordinates were placed in the same space reducing confounding errors (rotation and translation).

There have been several studies using PCA on either lateral skull radiographs or photographs. One of these studies assessed craniofacial form in 622 subjects and identified six PCs that explained 68 per cent of the variation. The study did not use Procrustes analysis to register the landmarks and arguably resulted in a rather complex array of facial parameters forming each PC (Cleall *et al.*, 1979). However, the first and third PCs were broadly similar to the findings in the present study, the first representing face height and the third convexity (mid-face and dental protrusion). The second component related to antero-posterior aspects of facial morphology, which is recorded in PC4 in the present study.

Photographs were used to identify six components explaining 86.5 per cent of the variance (Krey and Dannhauer, 2008). The first PC (33.9 per cent) described scaling along an axis from Porion to chin (a combination of vertical and horizontal vectors); the second component (28.6 per cent) characterized the vertical dimension of the lower face.

The soft tissue profiles of 170 patients aged 7–17 years were assessed (Halazonetis, 2007). The first eight PCs explained 90 per cent of the total shape variability. The first component (36 per cent) related to lip, nose, and chin prominence; the second component (18 per cent) related to facial convexity; and the next two components mainly related to lower lip shape. The overall shape differences between the average profiles of boys and girls were minor.

There were similarities and differences identified when making a comparison with previous studies. The present study was undertaken on a large cohort of the same age and previous studies have included subjects ranging from 7 years of age to adulthood. In addition, previous studies have used 2D records, whereas the 3D data utilized in this study should eliminate projection problems commonly found in radiographs and photographs (Houston *et al.*, 1986; Benson and Richmond, 1997). The chin prominence reported by Halazonetis (2007) and Krey and Dannhauer (2008) would be reported as a positive change in the *z*-axis for upper lip landmarks relative to the chin in PC4 of the current study, although this component only explains 5.3 per cent of the total variance.

As the 3D data were registered in a common space using Procrustes analysis, the derived PCs should be more valid based on relative importance of independent landmark coordinates in space. The 14 PCs derived from the current study reflect the complexity of facial morphology. The first three components describing face height, width, and convexity with the other 11 PCs contribute subtle changes to the face that makes the face unique.

The first PC (face height) explained 29 per cent of the variance and this evidence gives support to previous facial classifications as long/thin and short/wide faces (Schendel *et al.*, 1976; Opdebeeck and Bell, 1978; Opdebeeck *et al.*, 1978; Farkas, 1994). In this study, the average distance between the upper and the lower facial centroids (parameter P1) was 74.1 mm (ranging from 59.8 to 91.6 mm) with the nasion to pogonion distance at 101.7 mm (ranging from 82.8 to 127.6 mm). Male faces were on average 6 mm longer than female faces. This distance is slightly less than 8 mm reported for 50 fifteen-year-old Caucasians assessed by Farkas (1994) and higher than 1.8 mm for approximately 40 norms, 8- to 12-year old (Bugaighis *et al.*, 2011). In addition, previous clinical studies of long and short face types also reported limited samples, which reflect face heights equivalent to 2 SDs from the mean (Schendel *et al.*, 1976; Opdebeeck and Bell, 1978).

For PC2, the average distance between left and right centroids of the landmarks associated with the left and right eyes (parameter P2) was 61.5 mm (range 50.5–73 mm) with the average distance between the inner canthi of the eyes 34.2 mm (range 24.0–46.5 mm). The inter-canthal distance on average was 1.2 mm larger in males compared to females. Similar findings have been reported in smaller samples (Laestadius *et al.*, 1969; Farkas, 1994; Bugaighis *et al.*, 2011). Many syndromes exhibit abnormal inter-eye distance that may even exceed 2 SD from the mean (Feingold and

Bossert, 1974; Farkas *et al.*, 1989; Cohen *et al.*, 1995; Miamoto *et al.*, 2011); hypertelorism can be seen in 1q21.1 duplication syndrome, apert syndrome, basal cell nevus syndrome, Crouzon syndrome, DiGeorge syndrome, Noonan syndrome, and LEOPARD syndrome (Mann, 1957; Kreiborg and Cohen, 2010; Randolph *et al.*, 2011); and hypotelorism can be seen in patients with trigonocephaly (Nagasao *et al.*, 2011) and Schilbach–Rott syndrome (Joss *et al.*, 2002).

For PC3, the prominence of nose centroid (parameter P3) was on average 6.1 mm (ranging from −5.8 to 17.3 mm). The nasal tip protrusion (subnasale–pronasale) was on average slightly less in females (19.4 mm) compared to males (20.1 mm). Similar findings were reported elsewhere (Farkas, 1994; Zankl *et al.*, 2002).

Parameters P1, P2, and P3 associated with the first three PCs can be used to characterize the face as a 3D statistical continuum, where each coordinate corresponds to the standard deviation from the mean value of the respective parameter. Although male faces are generally larger than female faces (Ferrario *et al.*, 1998a,b, 1999), the PCAs for males and females show similar relative importance of facial parameters, which will be useful in facial classification.

Facial asymmetry has been suggested to arise from random variation or genetic and environmental influences (Waddington, 1957). The present study showed that minor facial asymmetry is relatively common in both sexes with similar patterns (PC8, nasal tip/columella base; PC9, nasal bridge; PC12, upper lip/philtrum; PC14, lower lip/chin). A mild degree of facial asymmetry has been reported elsewhere (Lu, 1965; Vig and Hewitt, 1975; Shah and Joshi, 1978; Alavi *et al.*, 1988; Peck *et al.*, 1991; Pirttiniemi, 1992; Ferrario *et al.*, 1993). Differences in facial asymmetry have been reported between the sexes; however, most of these studies have been undertaken on small samples (Farkas and Cheung, 1981; Ferrario *et al.*, 1994, 2001; Severt and Proffit, 1997; Shaner *et al.*, 2000; Smith, 2000; Haraguchi *et al.*, 2002; Hardie *et al.*, 2005; Ercan *et al.*, 2008).

In this study, the chin point (pogonion) deviated between −5.6 and 5.2 mm from the sagittal plane; nasal tip (pronasale), −4.7 and 4.9 mm, compared to the columella base (subnasale), −3.1 and 2.6 mm; glabella, −2.9 to 2.0 mm; nasion, −2.2 to 1.9 mm; upper lip (labiale superius), −2.3 and 2.5 mm; lower lip (labiale inferius), −1.5 to 2.8 mm. In previous studies, the degree of asymmetry has been attributed to discernible imbalances in the development of skeletal, dental, and soft tissues (Williamson and Simmons, 1979; Alavi *et al.*, 1988; Pirttiniemi *et al.*, 1990; Schmid *et al.*, 1991; Pirttiniemi, 1992). Unfortunately, the methods employed in these studies describe details of local imbalances with less emphasis on systematic assessment of facial asymmetry.

The current study provides a comprehensive range of soft tissue facial parameters for a population of 15.5-year-old Caucasians. The levels of deviation from the mean for the various parameters provide a basis for future assessment of subjects using craniofacial landmarks. Moreover, facial height and width have been reported to show strong genetic components (Savoye *et al.*, 1998; Baydas *et al.*, 2007) and it is intended to use the current data set in the future to explore genotype/phenotype associations through a genome-wide association study.

There are many projects underway around the world such as the FaceBase Consortium (Hochheiser *et al.*, 2011) collecting both 3D facial images and genetic data with the intention to undertake genome-wide association studies. It is important that the face data collected are standardized with matching age groups to allow analyses within and across population groups.

Conclusions

Fourteen PCs were identified for the total sample, which explained 82 per cent of the total variance in facial form, with the first three components accounting for 46 per cent of the variance. Similar results were identified for the data set when split into males and females, suggesting that the major components of facial variation do not differ between the genders. Variation in facial form can be accurately quantified and described as a multidimensional statistical continuum. This method of facial assessment may be useful to identify and classify faces and facial changes that occur as a result of growth and inform clinicians of appropriate healthcare interventions for specific facial types.

Funding

The UK Medical Research Council, the Wellcome Trust, and the Universities of Bristol and Cardiff provide core support for ALSPAC. Arshed M. Toma is funded by a Cardiff University 3-year PhD programme.

Acknowledgements

We are extremely grateful to all the families who took part in this study, the midwives for their help in recruiting them, and the whole ALSPAC team, which includes interviewers, computer and laboratory technicians, clerical workers, research scientists, volunteers, managers, receptionists, and nurses. Special thanks to Patricia Stewart and Susan Bryant for their great efforts in preparing the images.

References

Alavi D G, BeGole E A, Schneider B J 1988 Facial and dental arch asymmetries in Class II subdivision malocclusion. American Journal of Orthodontics and Dentofacial Orthopedics 93: 38–46

Baydas B, Erdem A, Yavuz I, Ceylan I 2007 Heritability of facial proportions and soft-tissue profile characteristics in Turkish Anatolian siblings. American Journal of Orthodontics and Dentofacial Orthopedics 131: 504–509

Benson P E, Richmond S 1997 A critical appraisal of measurement of the soft tissue outline using photographs and video. European Journal of Orthodontics 19: 397–409

Bookstein F L 1991 Morphometric tools for landmark data. Cambridge University Press, Cambridge

Bugaighis I, Mattick C, Tiddeman B, Hobson R 2011 Three-dimensional gender differences in facial form of children in the North East of England. European Journal of Orthodontics 2011 Apr 29 [Epub ahead of print] doi:10.1093/ejo/cjr033

Bugaighis I, O'Higgins P, Tiddeman B, Mattick C, Ben Ali O, Hobson R 2010 Three-dimensional geometric morphometrics applied to the study of children with cleft lip and/or palate from the North East of England. European Journal of Orthodontics 32: 514–521

Cleall J F, BeGole E A, Chebib F S 1979 Craniofacial morphology: a principal component analysis. American Journal of Orthodontics 75: 650–666

Cliff N 1988 The eigenvalues-greater-than-one rule and the reliability of components. Psychological Bulletin 103: 276–279

Cohen M M Jr, Richieri-Costa A, Guion-Almeida M L, Saavedra D 1995 Hypertelorism: interorbital growth, measurements, and pathogenetic considerations. International Journal of Oral and Maxillofacial Surgery 24: 387–395

Ercan I, *et al.* 2008 Facial asymmetry in young healthy subjects evaluated by statistical shape analysis. Journal of Anatomy 213: 663–669

Farkas L G 1994 Anthropometry of the head and face, 2nd edn. Raven Press, New York

Farkas L G, Cheung G 1981 Facial asymmetry in healthy North American Caucasians. An anthropometrical study. Angle Orthodontist 51: 70–77

Farkas L G, Ross R B, Posnick J C, Indech G D 1989 Orbital measurements in 63 hyperteloric patients. Differences between the anthropometric and cephalometric findings. Journal of Cranio-Maxillo-Facial Surgery 17: 249–254

Feingold M, Bossert W H 1974 Normal values for selected physical parameters: an aid to syndrome delineation. Birth Defects: Original Article Series 10: 1–16

Ferrario V F, Sforza C, Poggio C E, Schmitz J H 1998a Craniofacial growth: a three-dimensional soft-tissue study from 6 years to adulthood. Journal of Craniofacial Genetics and Developmental Biology 18: 138–149

Ferrario V F, Sforza C, Poggio C E, Schmitz J H 1998b Facial volume changes during normal human growth and development. Anatomical Record 250: 480–487

Ferrario V F, Sforza C, Poggio C E, Schmitz J H 1999 Soft-tissue facial morphometry from 6 years to adulthood: a three-dimensional growth study using a new modeling. Plastic and Reconstructive Surgery 103: 768–778

Ferrario V F, Sforza C, Poggio C E, Tartaglia G 1994 Distance from symmetry: a three-dimensional evaluation of facial asymmetry. Journal of Oral and Maxillofacial Surgery 52: 1126–1132

Ferrario V F, Sforza C, Ciusa V, Dellavia C, Tartaglia G M 2001 The effect of sex and age on facial asymmetry in healthy subjects: a cross-sectional study from adolescence to mid-adulthood. Journal of Oral and Maxillofacial Surgery 59: 382–388

Ferrario V F, Sforza C, Pizzini G, Vogel G, Miani A 1993 Sexual dimorphism in the human face assessed by euclidean distance matrix analysis. Journal of Anatomy 183: 593–600

Golding J, Pembrey M, Jones R, Team A S 2001 ALSPAC—the Avon Longitudinal Study of Parents and Children. I. Study methodology. Paediatric and Perinatal Epidemiology 15: 74–87

Guttman L 1954 Some necessary conditions for common factor analysis. Psychometrika 19: 149–161

Halazonetis D J 2007 Morphometric evaluation of soft-tissue profile shape. American Journal of Orthodontics and Dentofacial Orthopedics 131: 481–489

Hammond P, *et al.* 2005 Discriminating power of localized three-dimensional facial morphology. American Journal of Human Genetics 77: 999–1010

Hammond P, *et al.* 2004 3D analysis of facial morphology. American Journal of Medical Genetics Part A 126A: 339–348

Haraguchi S, Takada K, Yasuda Y 2002 Facial asymmetry in subjects with skeletal Class III deformity. Angle Orthodontist 72: 28–35

Hardie S, Hancock P, Rodway P, Penton-Voak I, Carson D, Wright L 2005 The enigma of facial asymmetry: is there a gender-specific pattern of facedness? Laterality 10: 295–304

Hennessy R J, Moss J P 2001 Facial growth: separating shape from size. European Journal of Orthodontics 23: 275–285

Hennessy R J, Kinsella A, Waddington J L 2002 3D laser surface scanning and geometric morphometric analysis of craniofacial shape as an index of cerebro-craniofacial morphogenesis: initial application to sexual dimorphism. Biological Psychiatry 51: 507–514

Hennessy R J, Baldwin P A, Browne D J, Kinsella A, Waddington J L 2007 Three-dimensional laser surface imaging and geometric morphometrics resolve frontonasal dysmorphology in schizophrenia. Biological Psychiatry 61: 1187–1194

Hennessy R J, Baldwin P A, Browne D J, Kinsella A, Waddington J L 2010 Frontonasal dysmorphology in bipolar disorder by 3D laser surface imaging and geometric morphometrics: comparisons with schizophrenia. Schizophrenia Research 122: 63–71

Hennessy R J, Lane A, Kinsella A, Larkin C, O'Callaghan E, Waddington J L 2004 3D morphometrics of craniofacial dysmorphology reveals sex-specific asymmetries in schizophrenia. Schizophrenia Research 67: 261–268

Hochheiser H, *et al.* 2011 The FaceBase Consortium: a comprehensive program to facilitate craniofacial research. Developmental Biology 355: 175–182

Houston W J, Maher R E, McElroy D, Sherriff M 1986 Sources of error in measurements from cephalometric radiographs. European Journal of Orthodontics 8: 149–151

Jackson D A 1993 Stopping rules in principal components analysis: a comparison of heuristical and statistical approaches. Ecology 74: 2204–2214

Joss S K, Paterson W, Donaldson M D, Tolmie J L 2002 Cleft palate, hypotelorism, and hypospadias: Schilbach-Rott syndrome. American Journal of Medical Genetics 113: 105–107

Kaiser H F 1958 The varimax criterion for analytic rotation in factor analysis. Psychometrika 23: 187–200

Kau C H, Richmond S 2008 Three-dimensional analysis of facial morphology surface changes in untreated children from 12 to 14 years of age. American Journal of Orthodontics and Dentofacial Orthopedics 134: 751–760

Kau C H, Richmond S 2010 Three-dimensional imaging for orthodontics and maxillofacial surgery. Wiley-Blackwell, London

Kau C H, Zhurov A, Scheer R, Bouwman S, Richmond S 2004 The feasibility of measuring three-dimensional facial morphology in children. Orthodontics and Craniofacial Research 7: 198–204

Kau C H, *et al.* 2005 Reliability of measuring facial morphology with a 3-dimensional laser scanning system. American Journal of Orthodontics and Dentofacial Orthopedics 128: 424–430

Kreiborg S, Cohen M M Jr 2010 Ocular manifestations of Apert and Crouzon syndromes: qualitative and quantitative findings. Journal of Craniofacial Surgery 21: 1354–1357

Krey K F, Dannhauer K H 2008 Morphometric analysis of facial profile in adults. Journal of Orofacial Orthopedics 69: 424–436

Laestadius N D, Aase J M, Smith D W 1969 Normal inner canthal and outer orbital dimensions. Journal of Pediatrics 74: 465–468

Lu K H 1965 Harmonic analysis of the human face. Biometrics 21: 491–505

Mann I 1957 Developmental abnormalities of the eye, 2nd edn. British Medical Association, London

McCance A M, Moss J P, Fright W R, James D R, Linney A D 1992 A three dimensional analysis of soft and hard tissue changes following bimaxillary orthognathic surgery in skeletal III patients. British Journal of Oral and Maxillofacial Surgery 30: 305–312

Miamoto C B, Soares R L, de Carvalho E M, Pereira L J, Marques L S 2011 Ocular hypertelorism in an orthodontic patient. American Journal of Orthodontics and Dentofacial Orthopedics 139: 544–550

Moss J P, Ismail S F, Hennessy R J 2003 Three-dimensional assessment of treatment outcomes on the face. Orthodontics and Craniofacial Research 6(Suppl. 1): 126–131; discussion 179–182

Nagasao T, Miyamoto J, Jiang H, Kaneko T, Tamaki T 2011 Biomechanical analysis of the effect of intracranial pressure on the orbital distances in trigonocephaly. Cleft Palate-Craniofacial Journal 48: 190–196

Nute S J, Moss J P 2000 Three-dimensional facial growth studied by optical surface scanning. Journal of Orthodontics 27: 31–38

Opdebeeck H, Bell W H 1978 The short face syndrome. American Journal of Orthodontics 73: 499–511

Opdebeeck H, Bell W H, Eisenfeld J, Mishelevich D 1978 Comparative study between the SFS and LFS rotation as a possible morphogenic mechanism. American Journal of Orthodontics 74: 509–521

Pearson K 1901 On lines and planes of closest fit to systems of points in space. Philosophical Magazine 2: 559–572

Peck S, Peck L, Kataja M 1991 Skeletal asymmetry in esthetically pleasing faces. Angle Orthodontist 61: 43–48

Pirttiniemi P 1992 Associations of mandibulofacial asymmetries, with special reference to glenoid fossa remodelling. University of Oulu, Oulu

Pirttiniemi P, Kantomaa T, Lahtela P 1990 Relationship between craniofacial and condyle path asymmetry in unilateral cross-bite patients. European Journal of Orthodontics 12: 408–413

Randolph J C, Sokol J A, Lee H B, Nunery W R 2011 Orbital manifestations of noonan syndrome. Ophthalmic Plastic and Reconstructive Surgery, 2011 Apr 1 [Epub ahead of print] doi:10.1097/IOP.0b013e318209976c

Savoye I, Loos R, Carels C, Derom C, Vlietinck R 1998 A genetic study of anteroposterior and vertical facial proportions using model-fitting. Angle Orthodontist 68: 467–470

Schendel S A, Eisenfeld J, Bell W H, Epker B N, Mishelevich D J 1976 The long face syndrome: vertical maxillary excess. American Journal of Orthodontics 70: 398–408

Schmid W, Mongini F, Felisio A 1991 A computer-based assessment of structural and displacement asymmetries of the mandible. American Journal of Orthodontics and Dentofacial Orthopedics 100: 19–34

Severt T R, Proffit W R 1997 The prevalence of facial asymmetry in the dentofacial deformities population at the University of North Carolina. International Journal of Adult Orthodontics and Orthognathic Surgery 12: 171–176

Shah S M, Joshi M R 1978 An assessment of asymmetry in the normal craniofacial complex. Angle Orthodontist 48: 141–148

Shaner D J, Peterson A E, Beattie O B, Bamforth J S 2000 Assessment of soft tissue facial asymmetry in medically normal and syndrome-affected individuals by analysis of landmarks and measurements. American Journal of Medical Genetics 93: 143–154

Smith W M 2000 Hemispheric and facial asymmetry: gender differences. Laterality 5: 251–258

Toma A M, Zhurov A, Playle R, Richmond S 2008 A three-dimensional look for facial differences between males and females in a British-Caucasian sample aged 151/2 years old. Orthodontics and Craniofacial Research 11: 180–185

Toma A M, Zhurov A, Playle R, Ong E, Richmond S 2009 Reproducibility of facial soft tissue landmarks on 3D laser-scanned facial images. Orthodontics and Craniofacial Research 12: 33–42

Vig P S, Hewitt A B 1975 Asymmetry of the human facial skeleton. Angle Orthodontist 45: 125–129

Waddington C H 1957 The strategy of the genes. George Allen and Unwin, London

Williamson E H, Simmons M D 1979 Mandibular asymmetry and its relation to pain dysfunction. American Journal of Orthodontics 76: 612–617

Zankl A, Eberle L, Molinari L, Schinzel A 2002 Growth charts for nose length, nasal protrusion, and philtrum length from birth to 97 years. American Journal of Medical Genetics 111: 388–391

Zhurov A, Kau C H, Richmond S 2005 Computer methods for measuring 3D facial morphology. In: Middleton J, Shrive M G, Jones M L (eds). Computer methods in biomechanics and biomedical engineering-5. First Numerics Ltd, Cardiff, pp. 2–7

Zhurov A I, Richmond S, Kau C H, Toma A 2010 Averaging facial images. In: Kau C H, Richmond S (eds). Three-dimensional imaging for orthodontics and maxillofacial surgery. Wiley-Blackwell, London, pp 126–144